37

# Telemanipulated Long Bone Fracture Reduction

Ralf Westphal[1], Simon Winkelbach[1], Thomas Gösling[2], Markus Oszwald[2], Tobias Hüfner[2], Christian Krettek[2] and Friedrich Wahl[1]
[1]*Institute for Robotics and Process Control,Technical University of Braunschweig,*
[2]*Department of Trauma Surgery, Hannover Medical School*
*Germany*

## 1. Introduction

Fractures of the human thigh bone, the femur, are commonly caused by high-energy injury mechanisms, like traffic accidents, predominantly in young males or by low-energy mechanisms, like falling, in elderly females (Martinet et al., 2000; Zlowodzki et al., 2006). With approximately 37 per 100,000 persons per year this is an extremely frequently encountered injury (Arneson et al., 1988; Zlowodzki et al., 2006). In 1999 334,410 patients with fractures of the lower extremities have been counted in Germany[1]. 144,659 of which had fractures of the thigh bone. After subtracting fractures in the proximal (hip side) femur, 25,695 patients remain with fractures in the femoral shaft (the middle, diaphyseal) region to which this work is dedicated.

Today, the treatment of choice for femur shaft fractures preferred by many surgeons is the minimal invasive technique of intramedullary nailing, which has been established as a standard technique for a definite stabilizing treatment in diaphyseal fractures of the lower extremities (Kempf et al., 1985; Krettek et al., 1996; Krettek, 2001; Winquist et al., 1984).

The complete process of intramedullary nailing is shown as a sketch in figure 1. The process starts with the opening of the medullary cavity. A small soft tissue cut of about 5 cm has to be placed at the proximal end of the femur. In extension of the femoral shaft, the bone's cavity has to be opened. This is achieved with a surgical drill. Now the intramedullary nail is inserted into the bone's medullary cavity until it reaches the fracture region. Subsequently the two major bone fragments are aligned accordingly to their correct anatomical position. For this the distal (knee side) fracture segment is moved by the surgeon by means of a so-called Schanz' screw, whereas the proximal fracture segment is hold in its position by means of a second Schanz' screw. According to (Rüedi & Murphy, 2000), this form of manipulation is called “joystick” reduction. When the fracture segments are finally aligned correctly, the intramedullary nail is further inserted. Finally the nail is locked with the bone by means of lateral screws. During the final insertion and the locking of the nail, the correct retention, which means maintaining the correct segment positions, has to be ensured. The whole process is supervised by means of X-ray imaging. A detailed description of this surgical procedure can be found in (Rüedi & Murphy, 2000).

[1] Source: Statistisches Bundesamt Deutschland (German Federal Statistical Office)

Source: Medical Robotics, Book edited by Vanja Bozovic, ISBN 978-3-902613-18-9, pp.526, I-Tech Education and Publishing, Vienna, Austria

Compared to open fracture reduction surgeries, in which the soft tissue around the fracture region is opened and the fracture segments are relocated and fixed with plates, this minimally invasive technique of intramedullary nailing has a number of advantages. It has proven high primary union rates of 90-99% while only having a very low incidence of surgery induced infection of <10% (Bhandari et al., 2000; Finkemeier et al., 2000; Kempf et al., 1985; Krettek et al., 1998; Winquist et al., 1984; Wolinsky et al., 1999).

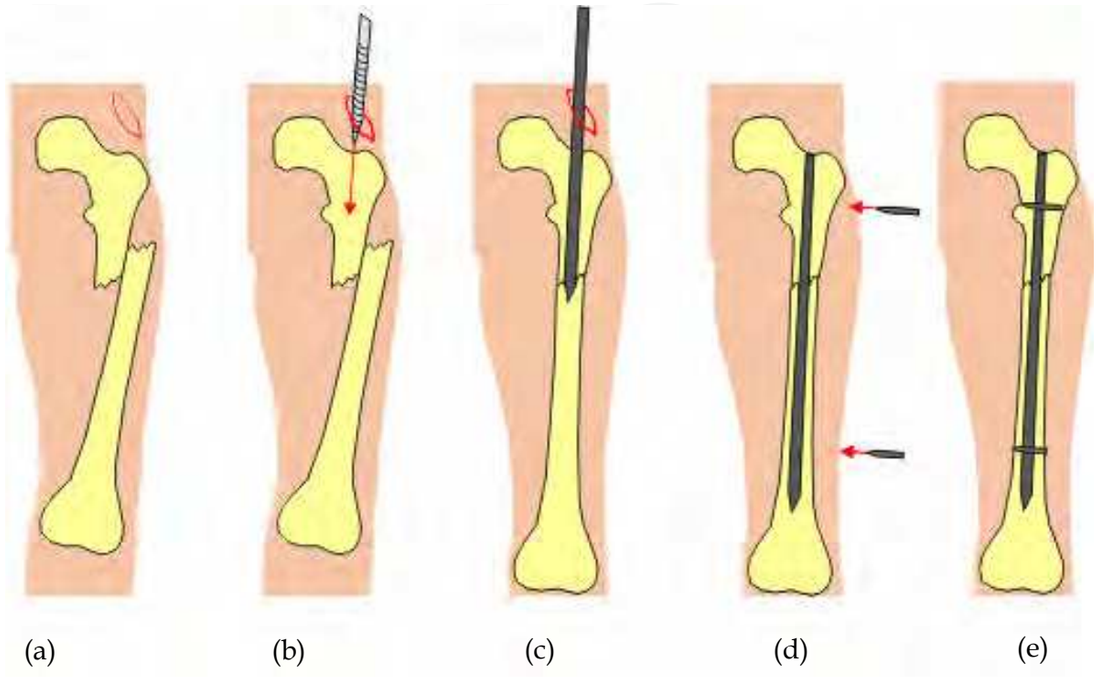


Figure 1. The process of closed intramedullary nailing (taken from (Winkelbach, 2006)) (a) Soft tissue cut at the hip. (b) Opening of the femur's medullary cavity. (c) Insertion of the intramedullary nail and reduction of the fracture. (d) Complete insertion of the nail which is locked by means of screws. (e) Result of the fracture reduction procedure

Besides its advantages, the closed intramedullary nailing also has a number of disadvantages, which are well-known in clinical practice and revealed in the open literature. Malalignment of the fracture segments is the most significant one which has a high impact on functional biomechanics. While being a personal tragedy for the patient, malalignment also has socio-economic effects as it leads to non-physiological conditions, which may result in a lengthened and costly rehabilitation during which the patient might be inhibited from working. In several cases even consecutive revision operations might become necessary.

A correct rotational alignment around the shaft axis is difficult to achieve, as intraoperatively only 2D fluoroscopy (X-ray imaging) is used for assessment. The limited visualization of structures on the bone surface and the limited display window are the main problems for achieving a correct rotational alignment. The frequent occurrence of rotational deviations of more than 10° is remarkable (Prevot et al., 1998; Winquist et al., 1984). Significant malalignment in the sagittal and frontal plane between 2% and 18% (Prevot et al., 1998; Winquist et al., 1984; Wolinsky et al., 1999)

and shortening of the femur by more than 2cm (Prevot et al., 1998; Winquist et al., 1984) are also reported.
The high radiation exposure to the patient and the operating staff is a second well-known problem. In open literature average X-ray image intensifier usage between 158 and 316 seconds is reported (Kempf et al., 1985; Sugarman et al., 1988). As the surgeon's hands are unprotected and close to the X-ray imaging field during the process of reduction, this is a particular point of criticism. Both problems, the malalignments and the high radiation exposure, are related to difficulties in achieving and maintaining the correct reduction. These problems are evidently specific for a long bone like the femur because of its tube-shaped anatomy and its counteracting muscle forces. Experiments performed during the course of our project revealed maximum forces of over 400 Newton during the reduction process (Gösling et al., 2006a; Gösling et al., 2006b; Gösling, 2007).
Accordingly, the aim of this interdisciplinary research project between the Hannover Medical School and the Technical University of Braunschweig is to support the described surgical procedure by developing and utilizing modern and emerging technologies like 3D imaging, surgical navigation, and robotics. The following objectives have been declared for the project:

- **Increased precision**: The overall precision of the fracture reductions should be increased. In particular, unacceptable reduction results with rotational deviations of 10 or more degrees, which might result in subsequent revision surgeries, should be averted.
- **Reduction of X-ray irradiation**: The number of X-ray images required to achieve the fracture reduction should be reduced. Especially for the operation staff, this point is highly desirable. Therefore not just simply reducing the number of X-ray images would be an advantage, but also the possibility to keep the operation staff away from the radiation during imaging.
- **Decreased operation time**: The possibility of decreasing the overall operation time would have two benefits. First, a shorter time of anesthesia means a reduction of the patient's stress. Second, from an economical point of view it would be desirable to shorten the operation times in order to reduce the overall costs. However, set-up time is often a crucial point for modern surgical procedures like navigation and especially robotics. So this point should be taken with care.

### 1.1 Related Work

Since its early beginnings in the mid 1980s, the research field of medical and in particular surgical robotics produced many different robotic systems for a wide variety of surgical applications. A complete review of this field will be beyond the scope of this paper, so we will just present research projects with a direct relation to the work presented in this paper. On the internet one can find an extensive database of surgical robotic systems (Pott, 2006). Further interesting reviews about research and development in this field can be found in (Cleary & Nguyen, 2003; Dario et al., 2003; Taylor & Joskowicz, 2002; Taylor & Stoianovici, 2003).
There is a world wide copious research in many different areas of surgical robotics, but only little work is done in the field of robotized fracture reduction. And so far, no commercially available robotic system exists, which supports fracture reduction procedures. Femoral

fracture reduction utilizing a robotic assistance system was first described by Bouazza-Marouf et al. in the year 1995 (Bouazza-Marouf et al., 1995). However, they just declared requirements for the reduction tool and did not publish anything about an implemented system or experimental results of fracture reductions performed by a robot.
The research group which worked on a project most similar to our group's work was the group of Nerlich, Monkman et al. from Regensburg, Germany (Füchtmeier et al., 2004). But as far as we know, their "RepoRobo" project has not been continued.
A second group which is working especially in the field of femur fracture reduction is the one headed by Warisawa from Tokyo, Japan. They follow the commendable approach of a non-invasive fracture reduction robot. Their robot system is attached to the patient's foot and performs respectively supports the reduction procedure in the femur via the knee joint. The only publication of this project we know from is from the year 2004 (Warisawa et al., 2004).
Seide et al. have been performing extensive research in developing a fracture reduction robotic system based on a parallel kinematic (a hexapod). Starting with purely manually actuated links (Seide & Wolter, 2000) where a software program computes the required link lengths, they have already performed successful clinical trials on patients with a completely automated actuated robotic system (Seide et al., 2004).
Another important research group is the one headed by Leo Joskowicz from The Hebrew University of Jerusalem, Israel. So far however, they haven't developed a robotic system for fracture reduction. Besides a robot for screw placement and distal locking their main contribution to CAS (Computer Assisted Surgery) in femoral fracture reduction is research on navigation (Hazan & Joskowicz, 2003; Joskowicz et al., 1998a; Joskowicz et al., 1998b; Yaniv et al., 1998).

### 1.2 Previous Work

Our first implementation of a surgical telemanipulator system for femur shaft fracture reduction, was a laboratory set-up in which artificial bones where used for the reduction process and CCD cameras where used to emulate intraoperative X-ray imaging. The good results of these tests, with very high reduction accuracies and short operation times, encouraged the further development of this telemanipulated fracture reduction concept. Furthermore, this pilot study revealed the importance of haptic and metric information to the surgeon during the reduction process (Gösling et al., 2005; Westphal et al., 2003; Westphal et al., 2004).
The next development step, was the telemanipulated reduction in a more realistic surgical environment. Using real X-ray images instead of CCD camera images and human specimens with intact soft tissues surrounding the broken femur bone, we were able to evaluate telemanipulated fracture reduction in an environment as close to clinical practice as possible. We could show, that telemanipulated fracture reduction in real human specimens is possible yielding overall satisfactory accuracies. It was shown that the required image intensifier usage could be reduced conspicuously, when compared with manually performed reductions. However, the accuracies obtained by the telemanipulator did not differ significantly from those obtained by the manual control group, so we couldn't show a definite benefit of the telemanipulated procedure in this set-up (Gösling, 2007; Westphal et al., 2006).

### 1.3 Contribution of this Work

As we have seen in our previous work, the telemanipulated reductions based on 2D X-ray imaging suffer from the same problems as the conventional manual reduction procedure: the limited view of the X-ray image and the low level of detail on the bone surface in the image. The way of interacting with the joystick has turned out to be a second weak point of the implemented telemanipulator system, as the operator had control over all three rotational degrees of freedom (DoFs) at the same time, while only having control over the two translational DoFs of the current X-ray viewing direction. Supporting all rotational DoFs at the same time using a joystick was shown to be not intuitively controllable by the operating surgeon. Therefore a more intuitive way of interaction is desirable.

The problems arising due to the low level of detail in the 2D X-ray images can be solved best by using high resolution 3D volume data, which can, for example, be obtained by computer tomography (CT) scanners or intraoperatively using motorized 3D C-arms. Therefore in this paper, a surgical telemanipulator system is presented, which uses a new and intuitive interaction principle based on a conventional joystick with force feedback capabilities and 3D imaging data. This telemanipulator system is evaluated extensively and successfully on human bones and complete human specimens.

The rest of the paper is organized as follows. In the next section, the telemanipulator system is described in detail, together with the experimental set-up, which was used for evaluation. Section 3 presents the results obtained by these experiments and section 4, finally gives a conclusion and an outlook on further research in the context of robotized fracture reductions.

## 2. Methods

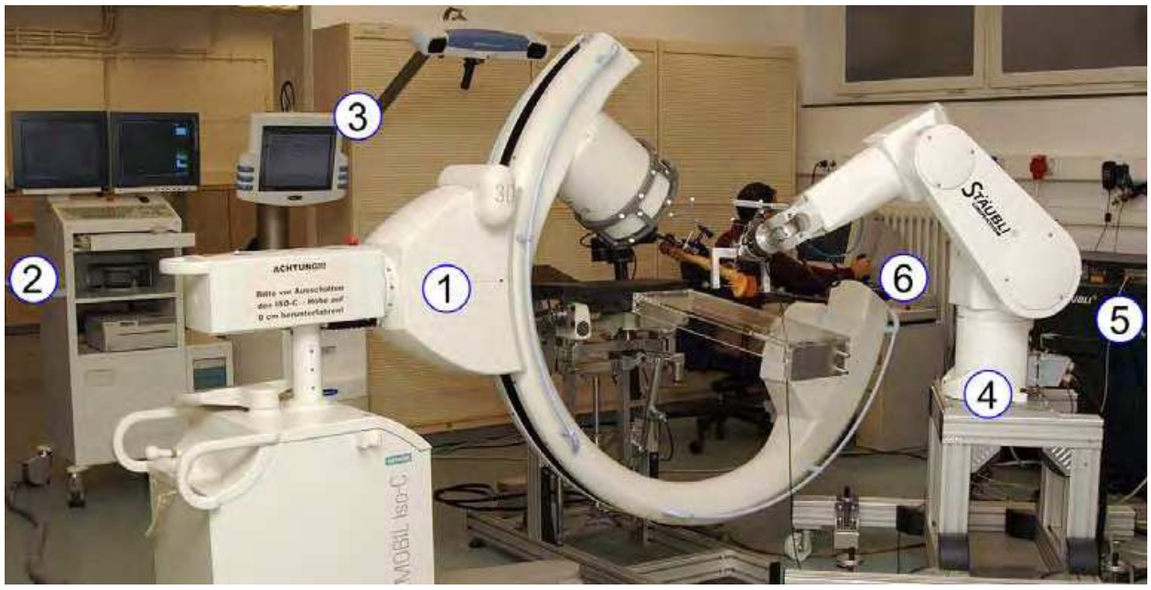


Figure 2. View of the 3D Telemanipulator set-up. 1: Fluoroscopy device. 2: Fluoroscopy workstation. 3: Surgical navigation system. 4: RX 90 robot. 5: Robot controller unit. 6: Controller PC

By using a telemanipulator system for supporting the fracture reduction process, the following benefits for the surgical procedure and for the surgeon can be expected.

- **Well-controlled motions**: A stable control of the fracture segment positions in all anatomical planes at the same time is difficult to achieve by the surgeon manually when using the conventional surgical method. But by ensuring a stable motion control, many control images and frequent reorientations of the fluoroscopic C-arm could be avoided, which would result in a reduction of X-ray exposure and a reduction of the risk of infection due to C-arm reorientations.
- **Fatigue-proof reduction and retention control**: In clinical pre-tests we measured forces and torques applied by the surgeon in order to achieve the fracture reduction (Gösling et al., 2006a; Gösling et al., 2006b; Gösling, 2007). These measurements revealed maximum peek forces of over 400 Newton. Obviously, under these conditions a human surgeon will have difficulties performing fine manipulations or keeping the retention over a longer period of time.
- **Keeping the surgeon distant to X-ray radiation**: In contrast to manually performed fracture reductions, the operation team can keep a distance from the X-ray device during imaging. Especially for the surgeon, who usually has his hands within or near the X-ray beam, this would result in a conspicuous reduction of the applied radiation dose.

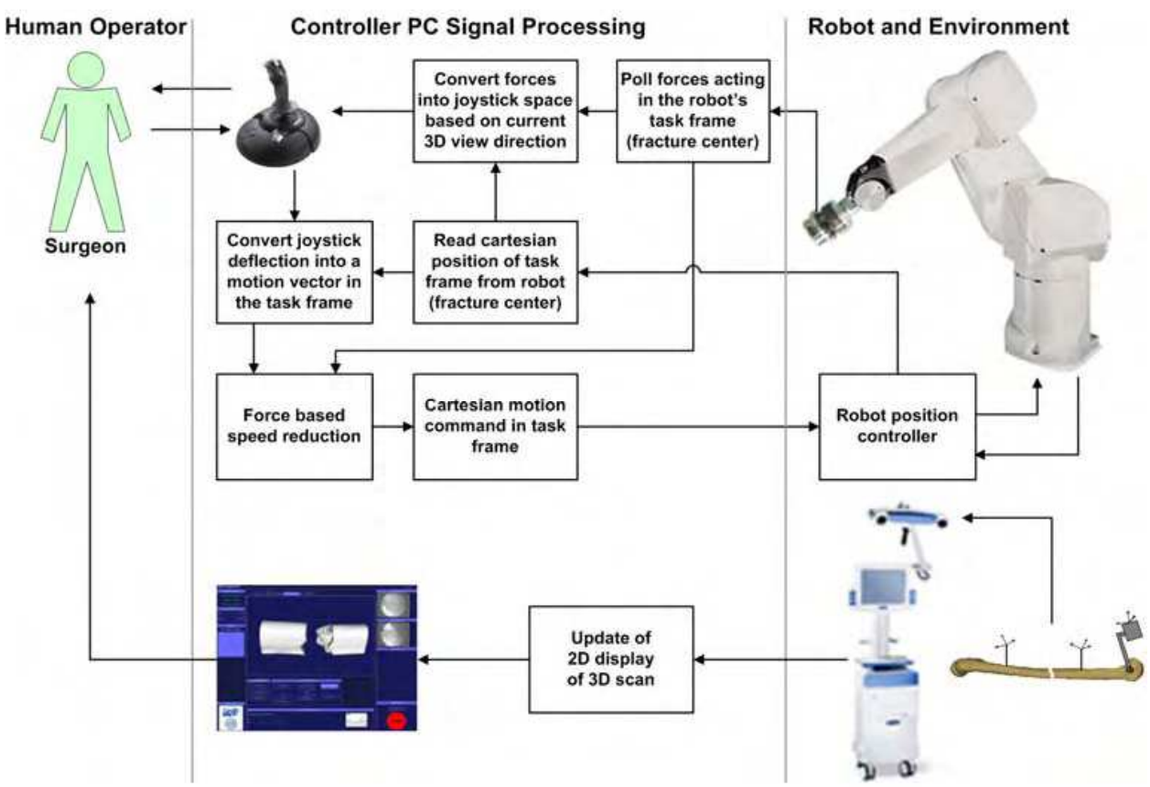


Figure 3. Signal flow diagram of the telemanipulator system during the fracture reduction process, illustrating interconnections between the surgeon, the controller PC, the robot, the force/torque sensor, and the navigation system

The telemanipulator set-up for robot assisted fracture reduction, developed by our work group, is shown in figure 2 and an overview of the system in figure 3. As can be seen in those images, our telemanipulator set-up uses an industrial robot, a Stäubli RX 90CR with its standard CS7B controller programmable in V+ (Stäubli Tec-Systems, Faverges, France). The robot is mounted on a wheeled platform so it can be placed besides the operation table. Furthermore, the robot is equipped with a force/torque sensor (FT Delta SI-660-60; Schunk, Lauffen, Germany) connected via an ISA card to a standard PC (Pentium® 4 2.8 GHz) running Microsoft® Windows® 2000. Intraoperative 3D imaging is achieved by the Siemens Siremobil Iso C 3D (Siemens AG, Medical Solutions, Erlangen, Germany) fluoroscopic C-arm. For the 3D tracking of the fracture segments and for the registration of the 3D image volume, we use an optical surgical navigation system (VectorVision, BrainLAB, Munich, Germany). The input device, a force feedback joystick (Microsoft®, SideWinder® ForceFeedback 2; Microsoft Corp., USA), is also connected to the PC. All four sub systems (PC, robot controller, navigation system, and fluoroscopic C-arm) are connected via a TCP/IP 100Mbit network.

### 2.1 Robotized Fracture Reduction

The process of fracture reduction is separated into two steps. The First step is the acquisition of a 3D DICOM data set and the reconstruction and registration of a 3D surface model, which is subsequently used for displaying a 3D scene on the PC. The second step is the reduction process itself.

At first, a 3D DICOM data set is acquired intraoperatively using the Siemens Iso C 3D C-arm. Within this 3D DICOM data set the bone has to be segmented from the surrounding soft tissue. This is performed simply by thresholding, with the threshold value being set manually by the surgeon. Next, 3D surface models are reconstructed from these segmented bone regions using the Marching Cube algorithm (Lorensen & Cline, 1987). This way surface geometries - meshes - are created for the two major fracture segments, the proximal and the distal part of the femur. For the smaller fragments, which in complex fractures may be located between the two major parts, no 3D meshes are generated, as they neither can be tracked nor manipulated by this telemanipulator approach. Both meshes have a local coordinate space in which the vertex positions are given. These coordinate spaces are defined in relation to the coordinate space of the DICOM data set. So we get the transformations ${}^{DICOM}\boldsymbol{T}_{PROX}$ and ${}^{DICOM}\boldsymbol{T}_{DIST}$ for the two meshes (table 1 summarizes all coordinate systems which are used in the following system description, as also illustrated in figure 4).

Having just these meshes of the fracture segments is not sufficient for being able to use them during navigated or telemanipulated surgeries. They need to be brought in relation to real world entities, i.e., to the current bone poses and to the robot. This process is called registration. The main application of registration algorithms in the field of computer assisted surgery is to bring preoperatively acquired data sets, like the ones from a CT scanner, in relation to an eventually changed intraoperative situation. In (Maintz, & Viergever, 1998; Zitova & Flusser, 2003) surveys on registration methods can be found. At this point it should just be noted, that the registration process can be simplified, if the data set is acquired intraoperatively, because then there is no need to deal with changes of the fracture segment poses between the preoperatively acquired data set and the intraoperative situation. Today, all major vendors of fluoroscopic C-arms have devices which are capable of acquiring such

3D data sets intraoperatively. The only prerequisite when using intraoperatively acquired 3D data sets is, that the objects which are represented in the data set can be set into relation with the coordinate space of the data set. Therefore, dynamic reference bases (DRBs) are rigidly mounted to the objects of interest, which are the proximal and distal fracture segments. These DRBs are visible to the navigation system during the acquisition of the 3D data set. The C-arm is equipped with infrared light reflecting elements as well; this way the 3D data set can be automatically set in relation to the DRBs by the navigation system. Figure 4 illustrates how the DRBs are mounted to the femur and which transformations are required in order to achieve the registration. The system uses three DRBs: the Y DRB, which is rigidly mounted to the proximal (hip side) fracture segment, the T DRB which is rigidly mounted to the distal (knee side) segment, and the SMS DRB which is mounted at the robot's hand. The surgical navigation system provides the robot controller program with the transformations between those three DRBs, namely ${}^{Y}\boldsymbol{T}_{T}$ and ${}^{Y}\boldsymbol{T}_{SMS}$. Additionally it obtains the pose of the 3D DICOM data set in relation to the DRBs at the time of the scan as transformation ${}^{Y}\boldsymbol{T}_{DICOM}$ between the world DRB and the DICOM data set. With this transformation, the registration of the two fracture meshes can be finalized in the following way.

$$ {}^{Y}\boldsymbol{T}_{PROX} = {}^{Y}\boldsymbol{T}_{DICOM} \cdot {}^{DICOM}\boldsymbol{T}_{PROX} \tag{1} $$

$$ {}^{T}\boldsymbol{T}_{DIST} = {}^{Y}\boldsymbol{T}_{T}^{-1} \cdot {}^{Y}\boldsymbol{T}_{DICOM} \cdot {}^{DICOM}\boldsymbol{T}_{DIST} \tag{2} $$

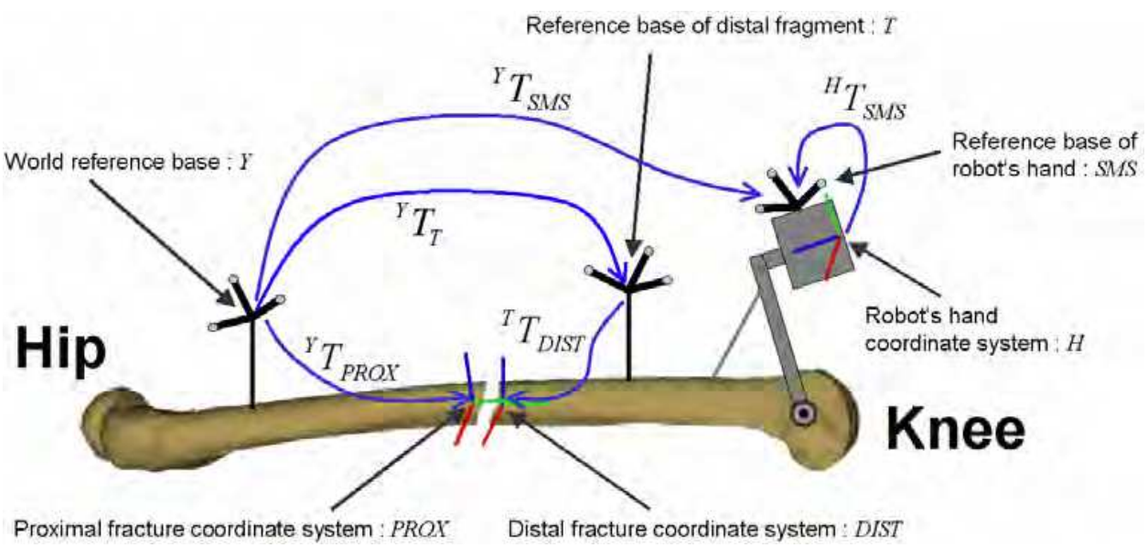


Figure 4. Registration of the intraoperative situation utilizing DRBs. The proximal DRB (left) is the world reference of the system, which is called the Y DRB. All other DRBs are given with respect to this DRB. The T DRB is the one rigidly mounted to the distal fracture segment. A third DRB, the SMS DRB, is mounted at the robot's hand with a fixed and known transformation ${}^{H}\boldsymbol{T}_{SMS}$ between them

The third DRB, the SMS DRB, is used to register the robot to the DICOM coordinate space and the fracture segments. The SMS DRB is mounted at a fixed and known position to the robot's hand. The rigid transformation between the robot's hand and the SMS DRB is given

as ${}^{H}\boldsymbol{T}_{SMS}$. Using the data from the surgical navigation system and the robot's hand pose ${}^{R}\boldsymbol{T}_{H}$, which can be obtained by the robot controller, the robot is registered to the surgical situs in the following way.

$$ {}^{Y}\boldsymbol{T}_{R} = {}^{Y}\boldsymbol{T}_{SMS} \cdot {}^{H}\boldsymbol{T}_{SMS}^{-1} \cdot {}^{R}\boldsymbol{T}_{H}^{-1} \tag{3} $$

We now describe the way the surgeon interacts with the robot by means of the joystick in order to perform the fracture reduction. The question is, how a 6D reduction problem (three translational and three rotational DoFs) can be solved efficiently by means of an input device with just two DoFs. The basic principle behind this is the reduction of the complex fracture reduction problem in 3D space to simpler reductions in 2D space. This is achieved by projecting the objects of the 3D world via standard computer graphics methods onto a 2D image plane. The reduction is now performed with respect to this 2D image with three DoFs. The interaction possibilities previously used for the 2D telemanipulator were simplified during the implementation of this 3D telemanipulator. While the translational way of interaction remains unchanged, the number of rotational DoFs controllable by the joystick was reduced. Only those rotational DoFs are controllable, which are "directly visible" from the current viewing direction: the rotation about an axis going through the fracture centre parallel to the viewing direction, and a rotation about the bone axis. In the translational motion mode the left/right and front/back deflections of the joystick are directly mapped to according translational motions of the distal fracture segment in the currently displayed viewing plane.

| | |
|---|---|
| Y[2] | The world reference coordinate system, which is defined by the DRB rigidly attached to the proximal fracture segment. |
| T[2] | The coordinate system of the DRB, which is rigidly attached to the distal fracture segment. |
| SMS[2] | The coordinate system of the DRB, which is rigidly attached to the robot's hand. |
| H | The coordinate system of the robot's hand. |
| R | The robot's base coordinate system. |
| DICOM | The coordinate system of the DICOM data set. |
| PROX | The fracture centre of the proximal fracture segment. |
| DIST | The fracture centre of the distal fracture segment. |
| JOY | The joystick coordinate system. |

Table 1. Coordinate systems used during robotized fracture reduction

In the rotational motion mode the front/back deflections are mapped to rotations about the bone axis, whereas the additional DoF of the joystick, the rotation about its own axis, is mapped to rotations of the distal fracture segment about an axis going through the fracture centre and resulting from the cross product of the view's up-vector and the bone axis. This vector is usually very close to an axis parallel to the current viewing direction, but facilitates a straight rotation path of the distal fracture segment in contrast to the curved path when rotating directly about the viewing direction. This is how the reduction can be performed in a 2D projection of the 3D scene. But how can the entire problem of a reduction in 3D space

[2] According to the DRB naming convention of the BrainLAB navigation system

be solved by this? This can be achieved by iteratively performing the 2D reduction described above from different viewing directions. Utilizing an additional switch on the joystick, the operator can pan the current viewing direction interactively to any arbitrary angle around the bone axis. Figure 5 illustrates this whole interaction principle.
When implementing this interaction mode, the coordinate space of the joystick has to be defined first, in which the two main DoFs of the stick (left/right and front/back deflection) are mapped to the X and Y axes. The additional DoF, the rotation about the stick's axis, is mapped to the Z axis. Therefore, a transformation matrix ${}^{DIST}\boldsymbol{T}_{JOY}$ has just to be found, which transforms the joystick's deflections into motions of the distal fracture segment. How can this transformation be obtained? Using the following notation for homogeneous transformation matrices,

$$\boldsymbol{T} = \begin{pmatrix} \boldsymbol{n}_x & \boldsymbol{o}_x & \boldsymbol{a}_x & \boldsymbol{p}_x \\ \boldsymbol{n}_y & \boldsymbol{o}_y & \boldsymbol{a}_y & \boldsymbol{p}_y \\ \boldsymbol{n}_z & \boldsymbol{o}_z & \boldsymbol{a}_z & \boldsymbol{p}_z \\ \boldsymbol{0} & \boldsymbol{0} & \boldsymbol{0} & \boldsymbol{1} \end{pmatrix} \tag{4}$$

the following equations have to be applied:

$$\vec{\boldsymbol{n}} = (\boldsymbol{0},\boldsymbol{1},\boldsymbol{0})^T \tag{5}$$

$$\vec{\boldsymbol{o}} = \vec{\boldsymbol{v}} \times \vec{\boldsymbol{n}} \tag{6}$$

$$\vec{\boldsymbol{a}} = \vec{\boldsymbol{n}} \times \vec{\boldsymbol{o}} \tag{7}$$

Where $\vec{\boldsymbol{v}}$ is the current viewing direction with respect to the distal fracture centre and the Y axis of the coordinate system corresponds with the bone axis. This results in the following homogeneous transformation matrix between the joystick coordinate system and the distal fracture centre:

$${}^{DIST}\boldsymbol{T}_{JOY} = \begin{pmatrix} \boldsymbol{0} & -\vec{\boldsymbol{v}}_z & \vec{\boldsymbol{v}}_x & \boldsymbol{0} \\ \boldsymbol{1} & \boldsymbol{0} & \boldsymbol{0} & \boldsymbol{0} \\ \boldsymbol{0} & \vec{\boldsymbol{v}}_x & \vec{\boldsymbol{v}}_z & \boldsymbol{0} \\ \boldsymbol{0} & \boldsymbol{0} & \boldsymbol{0} & \boldsymbol{1} \end{pmatrix} \tag{8}$$

Having this, a current joystick deflection $\vec{\boldsymbol{t}} = (\boldsymbol{d}_x, \boldsymbol{d}_y, \boldsymbol{0})^T$ for translational motions or $\vec{\boldsymbol{r}} = (\boldsymbol{d}_y, \boldsymbol{0}, \boldsymbol{dr}_z)^T$ (cp. figure 5) for rotational motions can be transformed into a motion command which can be executed with respect to the distal fracture centre.

$$\vec{\boldsymbol{t}}_{DIST} = \boldsymbol{s}_t \cdot \left({}^{DIST}\boldsymbol{T}_{JOY} \cdot \vec{\boldsymbol{t}}\right) \tag{9}$$

$$\vec{\boldsymbol{r}}_{DIST} = \boldsymbol{s}_r \cdot \left({}^{DIST}\boldsymbol{T}_{JOY} \cdot \vec{\boldsymbol{r}}\right) \tag{10}$$

Where $s_t$ and $s_r$ are scaling factors to scale the deflection values in the range [-100; 100] used in $\vec{t}$ and $\vec{r}$ to an appropriate value in mm or radian. From this the final transformation can be computed, which has to be applied to the distal fracture segment.

$$T_{move} = T_{trans}(\vec{t}_{DIST}) \cdot T_{rot_{vectr}}(\tilde{\vec{r}}_{DIST}, |\vec{r}_{DIST}|) \tag{11}$$

With

$$T_{trans}(\vec{t}) = \begin{pmatrix} 1 & 0 & 0 & \vec{t}_x \\ 0 & 1 & 0 & \vec{t}_y \\ 0 & 0 & 1 & \vec{t}_z \\ 0 & 0 & 0 & 1 \end{pmatrix} \tag{12}$$

$$T_{rot_{vctr}}(\vec{n}, \alpha) = \begin{pmatrix} \vec{n}_x^2 V\alpha + C\alpha & \vec{n}_x \vec{n}_y V\alpha - \vec{n}_z S\alpha & \vec{n}_x \vec{n}_z V\alpha + \vec{n}_y S\alpha & 0 \\ \vec{n}_x \vec{n}_y V\alpha + \vec{n}_z S\alpha & \vec{n}_y^2 V\alpha + C\alpha & \vec{n}_y \vec{n}_z V\alpha - \vec{n}_x S\alpha & 0 \\ \vec{n}_x \vec{n}_z V\alpha - \vec{n}_y S\alpha & \vec{n}_y \vec{n}_z V\alpha + \vec{n}_z S\alpha & \vec{n}_z^2 V\alpha + C\alpha & 0 \\ 0 & 0 & 0 & 1 \end{pmatrix} \tag{13}$$

Where $\tilde{\vec{r}}_{DIST}$ is the normalized vector of $\vec{r}_{DIST}$, $C\alpha = \cos(\alpha)$, $S\alpha = \sin(\alpha)$, and $V\alpha = vers(\alpha) = 1 - \cos(\alpha)$.

The viewing direction, i.e. the position of the camera, can be changed by the following formula in which $\alpha$ is the angle by which the viewing direction should be rotated around the femur axis. This angle is controlled by an additional switch on the joystick.

$${}^{Y}T_{CAM}^{new} = {}^{Y}T_{CAM}^{-1\ old} \cdot {}^{Y}T_{PROX} \cdot T_{rot_y}(\alpha) \cdot {}^{Y}T_{PROX}^{-1} \cdot {}^{Y}T_{CAM}^{old} \tag{14}$$

With

$$T_{rot_y}(\theta) = \begin{pmatrix} \cos(\theta) & 0 & \sin(\theta) & 0 \\ 0 & 1 & 0 & 0 \\ -\sin(\theta) & 0 & \cos(\theta) & 0 \\ 0 & 0 & 0 & 1 \end{pmatrix} \tag{15}$$

One of the main points of criticism of current telemanipulator systems, like the da Vinci system, is the lack of haptic feedback. Haptic feedback is of particular interest during orthopaedic surgeries, because the forces caused by the surrounding soft tissue or due to interfragmental contacts can become quite high and play an important role for motion planning during the reduction process. Therefore, the feedback of acting forces was identified as an important aspect for the development of a telemanipulator system supporting this kind of surgeries. The force feedback can in this case be simply seen as the inverse problem to the control of the distal fracture segment by means of a joystick. So one can simply use ${}^{DIST}T_{JOY}^{-1}$ to convert the forces measured in the fracture centre of the distal fracture segment into the coordinate axes of the joystick, whereas only the forces in X and Y direction are fed back to the joystick axes.

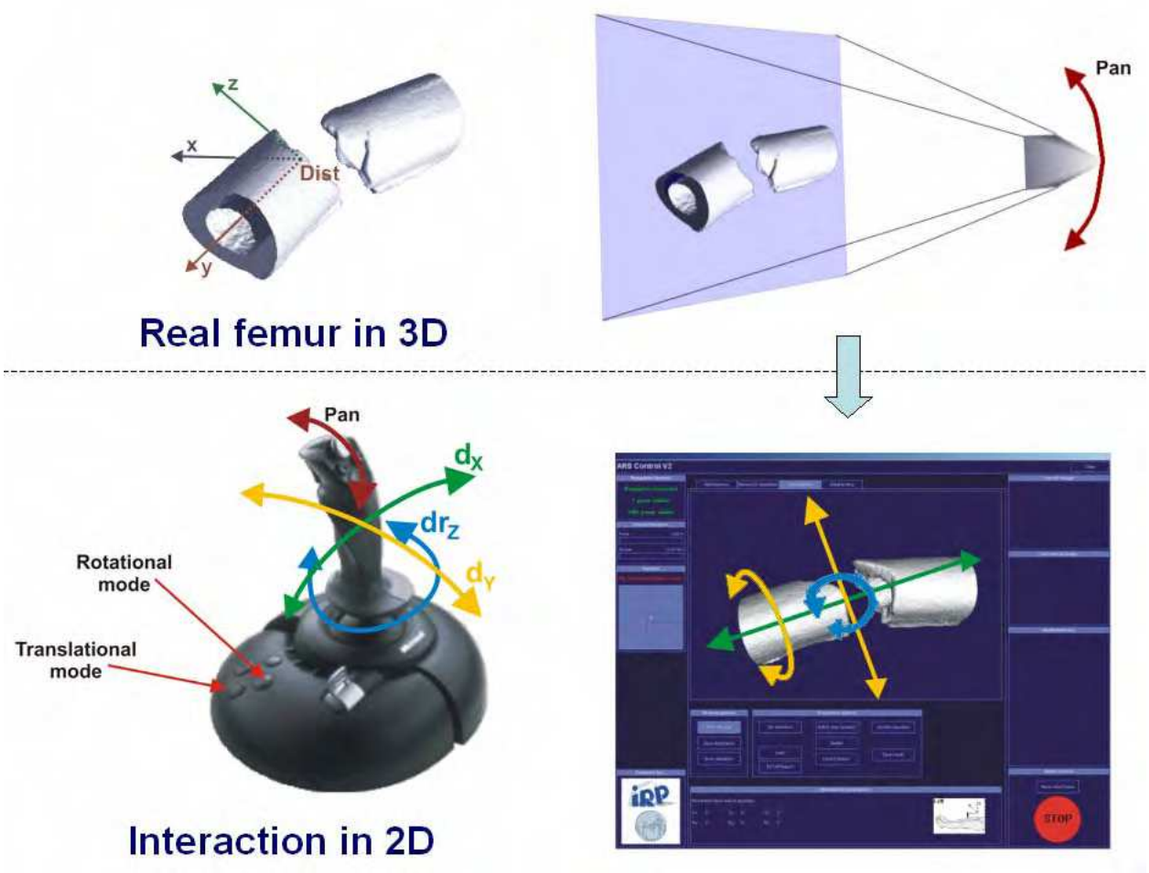


Figure 5. The interaction principle for telemanipulation based on 3D imaging data by means of a joystick with two DoFs. The surgeon can switch between rotational and translational manipulation mode. In every mode, he can control two DoFs with respect to the currently displayed viewing direction. The complete 3D reduction can be solved by performing the 2D reduction iteratively from different viewing directions. Therefore, the position from which the surgeon looks at the fracture site can be panned interactively around the bone axis to any arbitrary angle

### 2.2 Experiments

Figure 6 shows the process of the fracture reduction experiments carried out to evaluate the performance of telemanipulated fracture reductions based on 3D imaging data. The lower part of the procedure sequence presented in that figure could likewise be applied during real surgeries and can therefore be seen as a general procedure description for telemanipulated fracture reductions based on 3D imaging data.

First, two DRBs are mounted to the healthy bone in order to measure its unbroken reference transformation ${}^{Y}\boldsymbol{T}_{T}^{ref}$ . Next, the DRBs are removed, and a fracture is placed by means of a three-point-bending using a material testing machine. After remounting the DRBs to the broken bone parts, a 3D DICOM image data set is acquired with the IsoC 3D fluoroscopic C-arm. Resulting from the registration of this 3D data set, which is performed by the surgical navigation system, the transformations ${}^{T}\boldsymbol{T}_{DIST}$ and ${}^{Y}\boldsymbol{T}_{PROX}$ between the fracture segments

and the attached DRBs are obtained. From these transformations, the reference transformation between the fracture centres ${}^{PROX}\boldsymbol{T}_{DIST}^{ref}$ can be computed, utilizing ${}^{Y}\boldsymbol{T}_{T}^{ref}$.

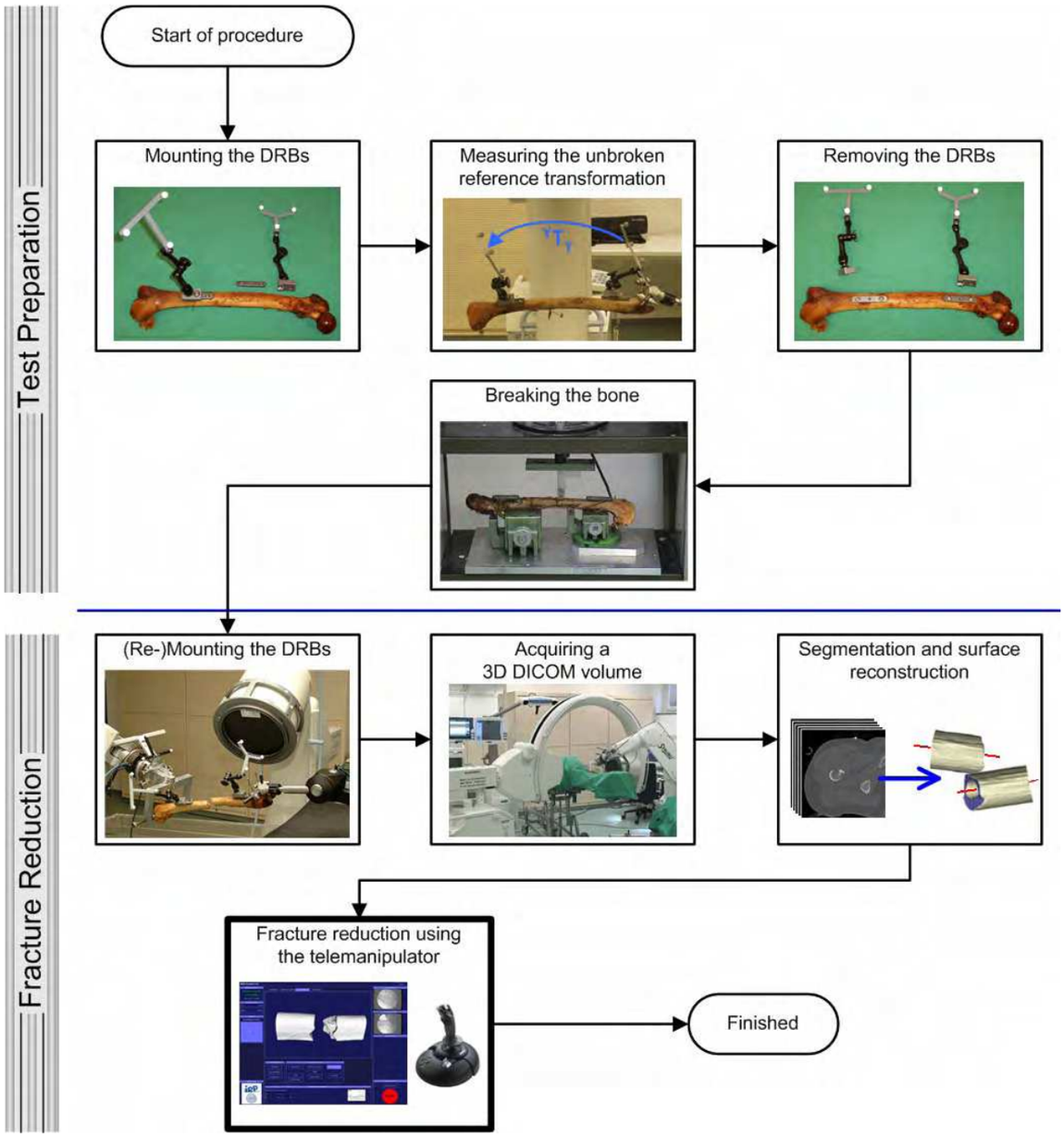


Figure 6. The process of telemanipulated reduction based on 3D imaging data. The upper "Test Preparation" part is only required for the test set-up. The lower part "Fracture Reduction" could likewise be used during real surgeries

Now the reduction is performed using the telemanipulator, controlled by means of the joystick as described before. As soon as the operator decides to finish the reduction process, the remaining deviations are computed based on the unbroken reference transformation and the current relative transformation between the two major fragments in the following way:

$$^{PROX}\boldsymbol{T}_{DIST}^{dev} = {}^{PROX}\boldsymbol{T}_{DIST}^{-1\ \ ref} \cdot {}^{Y}\boldsymbol{T}_{PROX}^{-1} \cdot {}^{Y}\boldsymbol{T}_{T} \cdot {}^{T}\boldsymbol{T}_{DIST} \tag{16}$$

Using this set-up 144 fracture reductions on 14 exposed human femurs - which means real bones without surrounding soft tissue - were performed by four different operators in order to measure learning curves and achievable reduction accuracies. 96 fracture reductions on 12 femurs of complete human specimens with intact soft tissue were performed in a second test series by the same four operators. This time, the results were also compared to reductions on 10 of the same 12 femurs performed in the conventional manual way by an experienced surgeon using 2D X-ray imaging only.

## 3. Results

The experiments with exposed bones achieved very good results with mean deviations of less than 2° and 2mm for simple fractures (AO fracture type A). Compared to manually performed reductions, these values are very satisfactory. Table 2 summarizes the results in detail. However, the achievable reduction accuracy decreases with increasing fracture complexity (AO fracture types B and C) as displayed in table 3. Expectedly, avoiding axial displacements is very difficult in complex fractures (AO fracture type C) without a direct connection between the two major fragments. But even for complex fractures an accuracy with mean rotational deviations of less than 4° was achieved overall.

| Parameter | Mean | Std. dev. | Min | Max |
|---|---|---|---|---|
| Reduction time (min:sec) | 4:34 | 2:31 | 2:00 | 12:57 |
| Lateral displacement (mm) | 1.61 | 1.23 | 0.16 | 4.80 |
| Axial displacement (mm) | 1.08 | 0.63 | 0.05 | 3.20 |
| Varus/valgus (left/right) (degrees) | 1.09 | 0.73 | 0.03 | 2.66 |
| Ante-/recurvature (front/back) (degrees) | 1.42 | 0.84 | 0.19 | 4.04 |
| Ex-/internal (axial) rotation (degrees) | 1.37 | 1.39 | 0.02 | 5.82 |

Table 2. Results of the telemanipulated reductions based on 3D imaging for simple fractures of the AO fracture type A on exposed bones (bones without soft tissue) (N=64)

| Parameter | Type A | Type B | Type C |
|---|---|---|---|
| Reduction time (min:sec) | 4:34 | 4:18 | 2:48 |
| Lateral displacement (mm) | 1.61 | 2.03 | 0.96 |
| Axial displacement (mm) | 1.08 | 2.35 | 5.55 |
| Varus/valgus (left/right) (degrees) | 1.09 | 2.18 | 1.32 |
| Ante-/recurvature (front/back) (degrees) | 1.42 | 2.02 | 2.28 |
| Ex-/internal (axial) rotation (degrees) | 1.37 | 2.37 | 3.89 |

Table 3. Mean values of the remaining deviations after telemanipulated fracture reduction based on 3D imaging for all three AO fracture types on exposed bones

Experiments on human specimens with intact surrounding soft tissue revealed similar results regarding accuracy and operation time. When compared to conventional manual fracture reductions on the same human femurs, the results obtained by the telemanipulated fracture reductions were significantly better than the ones achieved in the manual control group as can be seen in table 4. However, the operation time was lengthened during our experiments when using the telemanipulator system, which will be discussed in the conclusion.

| Parameter | Robot | Manual |
|---|---|---|
| Reduction time (min:sec) | 6:14 | 2:16 |
| Lateral displacement (mm) | 1.98 | 3.37 |
| Axial displacement (mm) | 2.00 | 3.69 |
| Varus/valgus (left/right) (degrees) | 1.11 | 2.53 |
| Ante-/recurvature (front/back) (degrees) | 1.24 | 1.85 |
| Ex-/internal (axial) rotation (degrees) | 2.89 | 8.42 |

Table 4. Mean values of the remaining deviations after fracture reduction for the telemanipulated reductions based on 3D imaging compared to conventional manual reductions based on 2D X-ray imaging in complete human specimens with intact soft tissue

## 4. Conclusion

The results obtained by the extensive experiments with the telemanipulator system clearly revealed the potential of robotic systems supporting fracture reduction of the femur. Not only is it possible to achieve very high accuracies in the reductions, but also the exposure of the operation team to X-ray radiation can be reduced, utilizing a robotic system in the presented way. The direct and well controlled motions of the robotically moved fracture segments might support a gentle reduction, when compared with manually performed reductions, which generally suffer from repetitive motions under high forces, implying high stress to the soft tissue surrounding the fracture. However, whether or not this really has an impact on the healthy soft tissue, will have to be proven in the future.

One further point is remarkable here. The operation time could not be reduced utilizing a robot as telemanipulator when compared to the manual control groups. Keeping in mind the experience from clinical practice this is a surprising result, because from the possibility of a direct and well defined motion control utilizing the robot in combination with high resolution and detailed 3D imaging data we would have expected to shorten the operation time significantly. So far we haven't been able to determine the reasons for this, but the surgeon who performed the manual control groups observed, that the rigid soft tissue situation in the formalin conserved specimens eases the reduction considerably. How this circumstance influences the telemanipulated reductions and the results obtained by it too, can only be hypothesized at this time. Future experiments on fresh cadavers with soft tissue properties very close to the real life surgical situation will have to be done in order to clarify this point.

The implemented way of visualizing the fracture and interacting with the robotic system by means of a simple input device with two main and one supplementary DoF has proven to be very efficient and intuitive for the surgeons, who performed the experiments. However, this input device has its limitations, as torques can not be fed back intuitively via its force feedback interface. Future work will have to be done in order to evaluate whether input devices with six DoFs for input as well as force/torque feedback might have the potential of further improving this telemanipulated robotic approach. In this context the evaluation of how much of the benefit of the present method is due to the 3D fracture visualization and how much is due to the robotized fracture reduction would be of interest, too. Comparing the robotized reductions with reductions manually performed but supported by a navigation system with 3D visualization capabilities like (Hazan & Joskowicz, 2003; Joskowicz et al., 1998a) can answer this question.

In contrast to the system presented in this paper, the fracture reduction robot presented by Warisawa et al. in (Warisawa et al., 2004) is more like a robotized traction table. They described, how the robot can be used as a "power assistant" device. The question of how a precise fracture reduction might be achieved with that robot was not answered adequately in their publication. The main problem in our opinion being the fixation of the robot to the patient's foot, which doesn't allow the bone segment in the femur to be controlled directly and predictably, as the articulated knee joint is still between the robot and the bone segment. While having the great advantage of being completely noninvasive, it might yield a lot of problems regarding control and achievable accuracy. We are going to address the problem of invasiveness in a different way, by trying to combine a noninvasive robot attachment with precise and well controlled bone manipulations in the future. A second very promising fracture reduction robot was developed by Seide et al. (Seide et al., 2004) based on an external fixateur with a parallel kinematic. The fracture reduction is performed automatically by this robot based on a pre-planned trajectory. The reduction is performed over a longer period of time - up to several days - which has the advantage of being very gentle to the soft tissue, as stated by the authors. However, the applicability of the system is limited to long bones. Even the applicability for fractures close to the joints, like proximal femur fractures with a higher incidence rate, might be questionable. The usage of a standard robotic architecture, as used in this paper, might be advantageous, as it is theoretically applicable for all kinds of bone fractures and we already performed successful fracture reductions in the proximal femur.
But still the results achievable with our telemanipulator system revealed the limitations of such an approach. The reduction accuracy degrades conspicuously with the complexity of the fracture. Especially for fractures of the fracture type C, without a direct connection between the two major fragments, larger translational as well as rotational deviations after reduction have to be expected.

### 4.1 Outlook

In this paper, only the telemanipulated reduction was presented. We have shown, that very precise reductions are possible, with such a telemanipulated approach. However, the remaining accuracy problems in more complex fracture types can be solved best by an automatic planning and reduction procedure according to figure 7. In order to achieve this, we already developed methods to automatically compute the desired and precise target transformations between the fracture segments (Winkelbach et al., 2003; Winkelbach, 2006). The required path planning and robot motion planning in order to achieve this automated reduction are to be published in (Westphal, 2007).
The surgical fixation of femoral fractures with an intramedullary nail comprises two procedure steps, during which the surgeon has to drill accurate holes into the patient's bone. The first hole opens the bone's medullary cavity so that the intramedullary nail can be inserted. The second drilling task is the final fixation of the nail by interlocking it by means of screws with the bone at the end of the surgical operation (distal locking). For both procedure steps, we developed automated image analysis methods, which can compute precise drilling trajectories. The robot is used as drill guidance system during these procedure steps (Westphal, 2007). Whereas each of these surgical tasks has been evaluated separately so far, the evaluation of the complete surgical workflow starting with the

robotized opening of the medullary cavity, following an automated reduction, finalized by a robotized distal locking is subject to our future work.

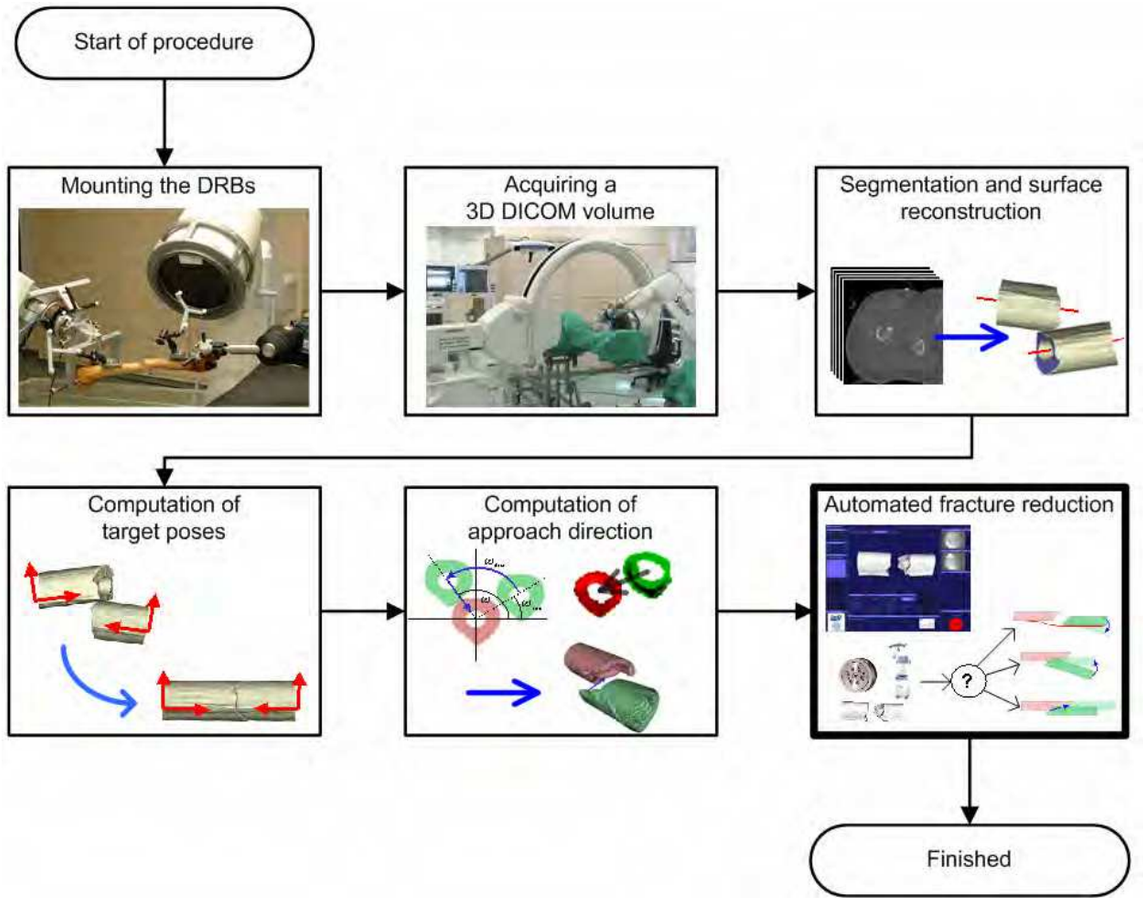


Figure 7. The process of automated fracture reduction based on 3D imaging data. After 3D data acquisition, segmentation, and surface reconstruction the desired target poses are computed automatically. A reduction motion plan is created, which is finally executed automatically under force/torque control by the robot

The generalization of the telemanipulation interaction principles presented herein for other fracture types is another topic, which is of interest both from a scientific and economic point of view. Basically the idea of reducing the complex 3D reduction problem to simple 2D reductions with intuitive and efficient visualization and interaction possibilities, is applicable for many fracture reduction problems, by simply extending the already proven conventional surgical procedures with the advantages of a robotized motion control. In order to evaluate this, our first laboratory set-up was adapted to perform reductions of hip fractures using plastic hips and again CCD cameras. The visualization and robot interaction was based on the three standardized 2D X-ray views, which are used by surgeons during conventional operations. As an extension to the femur fracture interaction principle we had to introduce a second centre of rotation, so the surgeon can decide interactively whether the dorsal or ventral fracture zone should be retained during rotations. Though the results of

these tests have been very satisfactory (Hüfner et al., 2003), we have not extended research in this direction so far. However, we belief that further research would be worthwhile.

## 5. Acknowledgements

We would like to thank BrainLAB (Munich, Germany) for supporting us with an interface to their navigation system and the AO-Developing-Institute (ADI, Davos, Switzerland) for lending us their pneumatic fixation device. We thank the Department of Anatomy of the Hannover Medical School for making specimens available for our experiments. Finally, we thank the German Research Foundation (DFG) for funding this project under the grants WA 848/10-1/2 and KR 2161/1-1/2 "Roboterunterstützte Femurmarknagelung".

## 6. References

Arneson, T.; Melton, L. 3rd.; Lewallen, D. & O'Fallon, W. (1988). Epidemiology of diaphyseal and distal femoral fractures in Rochester, Minnesota, 1965-1984, In: *Clin Orthop Relat Res*, Vol. 234, pp. 188-94

Bhandari, M.; Guyatt, G.; Tong, D.; Adili, A. & Shaughnessy, S. (2000). Reamed versus nonreamed intramedullary nailing of lower extremity long bone fractures: a systematic overview and meta-analysis, In: *J Orthop Trauma*, Vol. 14, No. 1, pp. 2-9

Bouazza-Marouf, K.; Browbank, I. & Hewit, J. (1995). Robotic-assisted internal fixation of femoral fractures, In: *Proc.Inst.Mech.Eng*, pp. 51-58

Cleary, K. & Nguyen, C. (2003). Medical robotics. In: *Biomedical Technology and Devices Handbook*, Moore, J. & Zouridakis, G. (ed), CRC Press, chapter 32

Dario, P.; Hannaford, B. & Menciassi, A. (2003). Smart Surgical Tools and Augmenting Devices, In: *IEEE Transactions on Robotics and Automation*, Vol. 19, No. 5, October , pp. 782-792

Finkemeier, C.; Schmidt, A.; Kyle, R.; Templeman, D. & Varecka, T. (2000). A prospective, randomized study of intramedullary nails inserted with and without reaming for the treatment of open and closed fractures of the tibial shaft, In: *J Orthop Trauma*, Vol. 14, No. 3, pp. 187-93

Füchtmeier, B.; Egersdoerfer, S.; Mai, R.; Hente, R.; Dragoi, D.; Monkman, G. & Nerlich, M. (2004). Reduction of femoral shaft fractures in vitro by a new developed reduction robot system 'RepoRobo', In: *Injury, Int. J. Care Injured*, 35, pp. A113-A119

Gösling, T.; Westphal, R.; Hüfner, T.; Faulstich, J.; Kfuri, M.; Wahl, F. & Krettek, C. (2005). Robot-assisted fracture reduction: A preliminary study in the femur shaft. In: *Med. Biol. Eng. Comput*., Vol. 43, pp. 115-120

Gösling, T.; Hüfner, T.; Westphal, R.; Faulstich, J.; Hankemeier, S.; Wahl, F. & Krettek, C. (2006). Overdistraction of the fracture eases reduction in delayed femoral nailing: results of intraoperative force measurements. In: *J Trauma*, Vol. 61, No. 4, October, pp. 900-4

Gösling, T.; Westphal, R.; Faulstich, J.; Sommer, K.; Wahl, F.; Krettek, C. & Hüfner, T. (2006). Forces and torques during fracture reduction: Intraoperative measurements in the femur, In: *J Orthop Res*, Vol. 24, No. 3, January, pp. 333-338

Gösling, T. (2007). *Die roboterassistierte Reposition von Schaftfrakturen - Grundlagenversuche am Femur*, Department of Trauma Surgery, Hannover Medical School, Habil.

Hazan, E. & Joskowicz, L. (2003). Computer-assisted image-guided intramedullary nailing of femoral shaft fractures, In: *Techniques in Orthopaedics*, Special Issue on Computer-Aided Orthopaedic Surgery, Vol. 18, No. 2, pp. 130-140

Hüfner, T.; Westphal, R.; Gösling, T.; Wahl, F.; Kfuri, M. Jr. & Krettek, C. (2003). Roboterassistierte Beckenreposition. In: *CURAC 2003, Computer und Roboter Assistierte Chirurgie*

Joskowicz, L.; Milgrom, C.; Simkin, A.; Tockus, L. & Yaniv, Z. (1998). FRACAS: a system for computer-aided image-guided long bone fracture surgery, In: *Computer-Aided Surgery*, Vol. 3, No. 6, May

Joskowicz, L.; Tockus, L.; Yaniv, Z.; Simkin, A. & Milgrom, C. (1998). Computer-aided image-guided bone fracture surgery: concept and implementation, In: *12th Int. Symp. on Computer Assisted Radiology and Surgery*, Lemke et al (Ed.), Elsevier

Kempf, I.; Grosse, A. & Beck, G. (1985). Closed locked intramedullary nailing. Its application to comminuted fractures of the femur. In: *J.Bone Joint Surg.Am.*, Vol. 67, pp. 709-720

Krettek, C.; Gluer, S.; Schandelmaier, P. & Tscherne, H. (1996). Marknagelung offener Frakturen. In: *Orthopade*, Vol. 25, pp. 223-233

Krettek, C.; Schandelmaier, P. & Tscherne, H. (1998). Treatment of femoral shaft fractures with an unreamed solid nail (UFN) and standard locking, In: *Operat.Orthop.Traumatol*, Vol. 6, pp. 179-192

Krettek, C. (2001). Prinzipien der intramedullären Knochenbruchstabilisierung. Teil 2: Operationstechnik. In: *Unfallchirurg*, Vol. 104, pp. 749-769

Lorensen, W. E. & Cline, H. E. (1987). Marching Cubes: A High Resolution 3D Surface Construction Algorithm. In: *Computer Graphics (Proceedings of SIGGRAPH '87)*, Vol. 21, pp. 163-169

Maintz, J. & Viergever, M. (1998). A survey of medical image registration. In: *Medical Image Analysis 2*, No. 1, pp. 1-36

Martinet, O.; Cordey, J.; Harder, Y.; Maier, A.; Buhler, M. & Barraud, G. (2000). The epidemiology of fractures of the distal femur, In: *Injury*, Vol. 31, Suppl 3, pp. C62-3

Pott, P. P. (2006). *MERODA, the MEdical RObotics DAtabase*. http://www.ma.uni-heidelberg.de/apps/ortho/meroda/, cited: 18. Jul. 2007

Prevot, N.; Charissoux, J.; Fiorenza, F.; Arnaud, J. & Pecout, C. (1998). Utilisation d'un clou non fendu de Russel-Taylor pour la stabilisation des fractures du femur. A propos de 57 fractures avec 30 etudes tomodensitometriques de la rotation. In: *Rev Chir Orthop Reparatrice Appar Mot*, Vol. 84, pp. 33-40

Rüedi, T. & Murphy, W. (2000). *AO Principles of Fracture Management*, Thieme

Seide, K. & Wolter, D. (2000). Korrekturen mit dem Hexapoden, In: *Orthopäde*, 29, pp. 39-46

Seide, K.; Faschingbauer, M.; Wenzl, M.; Weinrich, N. & Juergens, C. (2004). A hexapod robot external fixator for computer assisted fracture reduction and deformity correction, In: *Int. J. Medical Robotics and Computer Assisted Surgery*, Vol. 1, No. 1, pp. 64-69

Sugarman, I.; Adam, I. & Bunker, T. (1988). Radiation dosage during AO locking femoral nailing. In: *Injury*, Vol. 19, pp. 336-338

Taylor, R. & Joskowicz, L. (2002). Computer-integrated surgery and medical robotics. In: *Standard Handbook of Biomedical Engineering and Design*, Kutz, M. (ed), 1st Edition. McGraw-Hill Professional, pp. 325-353

Taylor, R. & Stoianovici, D. (2003). Medical robotics in computer-integrated surgery. In: *IEEE Transactions on Robotics and Automation*, Vol. 19, No. 5, Oct., pp. 765-781

Warisawa, S.; Ishizuka, T.; Mitsuishi, M.; Yonenobu, K.; Sugano, N. & Nakazawa, T. (2004). Development of a femur fracture reduction robot, In: *ICRA 2004 - IEEE International Conference on Robotics and Automation*.

Westphal, R.; Faulstich, J.; Gösling, T.; Winkelbach, S.; Hüfner, T.; Krettek, C. & Wahl, F. (2003). Fracture reduction using a telemanipulator with haptical feedback. *CARS 2003, Proceedings of the 17th International Congress and Exhibition, Computer Assisted Radiology and Surgery*, International Congress Series 1256, June 25-28, London, UK, Elsevier, Amsterdam, p. 1369

Westphal, R.; Winkelbach, S.; Finkemeyer, B.; Wahl, F.; Gösling, T.; Hüfner, T.; Faulstich, J. & Krettek, C. (2004). Progress in Robot Assisted Fracture Reduction. *Video-Proceedings - IEEE, International Conference on Robotics and Automation*, April 26-30, New Orleans, USA

Westphal, R.; Winkelbach, S.; Gösling, T.; Hüfner, T.; Faulstich, J.; Martin, P.; Krettek, C. & Wahl, F. (2006). A Surgical Telemanipulator for Femur Shaft Fracture Reduction, In: *Int. J. of of Medical Robotics and Computer Assisted Surgery*, Vol. 2, No. 3, pp. 238-50

Westphal, R. (2007). Fortschritte in der Robotik: Sensor-based Surgical Robotics: Contributions to Robot Assisted Fracture Reduction, (to be published), Shaker-Verlag, *Dissertation*

Winquist, R.; Hansen, S. Jr. & Clawson, D. (1984). Closed intramedullary nailing of femoral fractures. A report of five hundred and twenty cases, In: *J.Bone Joint Surg.Am.*, Vol. 66, pp. 529-539

Winkelbach, S. ; Westphal, R. & Gösling, T. (2003). Pose Estimation of Cylindrical Fragments for Semi-automatic Bone Fracture Reduction, In: *Pattern Recognition (DAGM 2003)*, *Lecture Notes in Computer Science*, Michaelis, B. & Krell, G. (ed), Vol. 2781, Springer, September, pp. 566-573

Winkelbach, S. (2006). Fortschritte in der Robotik. vol. 10: Das 3d-Puzzle-Problem - Effiziente Methoden zum paarweisen Zusammensetzen von dreidimensionalen Fragmenten, Shaker-Verlag, *Dissertation*

Wolinsky, P.; McCarty, E.; Shyr, Y. & Johnson, K. (1999). Reamed intramedullary nailing of the femur: 551 cases. In: *J.Trauma*, Vol. 46, pp. 392-399

Yaniv, Z.; Joskowicz, L.; Simkin, A.; Garza-Jinich, M. & Milgrom, C. (1998). Fluoroscopic image processing for computer-aided orthopaedic surgery, In: *1st Int. Conf. on Medical Computing and Computer-Assisted Intervention*, Grimson et al. (Ed.), Lecture Notes in Computer Science, Springer

Zitova, B. & Flusser, J. (2003). Image registration methods: a survey. In: *Image and Vision Computing*, Vol. 21, No. 11, pp. 977-1000

Zlowodzki, M.; Bhandari, M.; Marek, D.; Cole, P. & Kregor, P. (2006). Operative treatment of acute distal femur fractures: systematic review of 2 comparative studies and 45 case series (1989 to 2005), In: *J Orthop Trauma,* Vol. 20, No. 5, pp. 366-71


**Medical Robotics**

Edited by Vanja Bozovic

ISBN 978-3-902613-18-9
Hard cover, 526 pages
**Publisher** I-Tech Education and Publishing
**Published online** 01, January, 2008
**Published in print edition** January, 2008

The first generation of surgical robots are already being installed in a number of operating rooms around the world. Robotics is being introduced to medicine because it allows for unprecedented control and precision of surgical instruments in minimally invasive procedures. So far, robots have been used to position an endoscope, perform gallbladder surgery and correct gastroesophogeal reflux and heartburn. The ultimate goal of the robotic surgery field is to design a robot that can be used to perform closed-chest, beating-heart surgery. The use of robotics in surgery will expand over the next decades without any doubt. Minimally Invasive Surgery (MIS) is a revolutionary approach in surgery. In MIS, the operation is performed with instruments and viewing equipment inserted into the body through small incisions created by the surgeon, in contrast to open surgery with large incisions. This minimizes surgical trauma and damage to healthy tissue, resulting in shorter patient recovery time. The aim of this book is to provide an overview of the state-of-art, to present new ideas, original results and practical experiences in this expanding area. Nevertheless, many chapters in the book concern advanced research on this growing area. The book provides critical analysis of clinical trials, assessment of the benefits and risks of the application of these technologies. This book is certainly a small sample of the research activity on Medical Robotics going on around the globe as you read it, but it surely covers a good deal of what has been done in the field recently, and as such it works as a valuable source for researchers interested in the involved subjects, whether they are currently “medical roboticists” or not.



INTECH
open science | open minds

**InTech Europe**
University Campus STeP Ri
Slavka Krautzeka 83/A
51000 Rijeka, Croatia

**InTech China**
Unit 405, Office Block, Hotel Equatorial Shanghai
No.65, Yan An Road (West), Shanghai, 200040, China
中国上海市延安西路65号上海国际贵都大饭店办公楼405单元

Phone: +385 (51) 770 447
Fax: +385 (51) 686 166
www.intechopen.com

Phone: +86-21-62489820
Fax: +86-21-62489821



IntechOpen

IntechOpen